International Journal of Recent Trends in Science And Technology, P-ISSN 2277-2812 E-ISSN 2249-8109
Special Issue, ACAEE: 2018 pp 199-202

Original Research Article

Upconversion and quantum cutting emission in Y_2O_3 co-doped Ho^{3+} and Yb^{3+} oxide phosphor synthesized by solution route: A comparative study

Prachi Tadge[1*], Sudeshna Ray[2]

[1]Research Scholar, [2]Associate Professor, AISECT University, Bhopal, Madhya Pradesh, INDIA.
Email: praachidhote.89@gmail.com

Abstract

We have carried out a comparative study of Upconversion (UC), and Quantum Cutting (QC) emission of rare-earth ions Ho^{3+} and Yb^{3+} codoped Y_2O_3 host. An efficient Near-Infrared Quantum Cutting and Upconversion has been demonstrated in Ho^{3+} and Yb^{3+} co-activated Y_2O_3 sample, synthesized by a complex based precursor solution method. The Upconversion emission excited with 980 nm and Quantum Cutting emission excited with 362 nm and 449 nm, of (1%) Ho^{3+} and (x %) Yb^{3+} with (x % = 0, 5, 10, 20, 30, 50) codoped Y_2O_3 samples, reveals the efficient emission in the green region which corresponds to $^5S_2$–$^5I_8$ transition of Ho^{3+} at 549 nm in visible region. Furthermore, the Ho^{3+} emission for Upconversion is 4.27 times higher than that for Quantum Cutting emission, peak at 549 nm. The faster decline of life-time corresponding to time of the $^5S_2$–$^5I_8$ transition of Ho^{3+}, from 93 ms at 362 nm and 96 ms at 449 nm in single doped sample to 11 ms in 30% Yb^{3+} codoped sample accompanied by the change in the nature of decay-time curves from single exponential to non-single-exponential, clearly reflect the occurrence of Quantum Cutting Phenomenon in the codoped samples. The Upconversion decay also a show life-time corresponding to the $^5S_2$–$^5I_8$ transition of Ho^{3+}, from 109 ms at 980 nm in single doped sample to 62 ms in 30% Yb^{3+} codoped sample. The energy transfer from Ho^{3+} to Yb^{3+} inY_2O_3:Ho^{3+} (1%), Yb^{3+} (20%) sample has been calculated to be 72.91% and the corresponding Quantum Cutting Efficiency was calculated to be 172.91%. From the life time measurement, Energy Transfer Efficiency and the rate of Energy Transfer with respect to Yb^{3+} concentration have been evaluated. The results reveal that application of these phosphors may improve the conversion efficiency of DSSCs.

Key Words: Upconversion, Quantum Cutting, Dye Sensitized solar cell (DSSCs).

[*]Address for Correspondence:
Dr. Prachi Tadge, Research Scholar, AISECT University, Bhopal, Madhya Pradesh, INDIA.
Email: praachidhote.89@gmail.com

Access this article online
Quick Response Code:
Website:
www.statperson.com
Accessed Date:
26 March 2018

INTRODUCTION

State-of the- art commercial crystalline Si (c-Si) solar cells dominate the market and have energy efficiencies around 15%.[2] The main source of energy loss (over 70%) is related to the spectral mismatch of incident solar photon energies to the energy gap (Eg) of a solar cell.[3] Solar cells generate a single electron–hole pair upon absorbing a photon above the bandgap.[4] Photons with energies lower than the bandgap are not absorbed, and for photons with energies exceeding the bandgap, the excess energy is lost as heat during the fast thermalization of the 'hot' charge carriers. Taking these sources of energy loss into account, the maximum energy efficiency that can be reached is known as the Shockley–Queisser limit.[5] For the solar spectrum, the limit is 30% for a solar cell with a bandgap of 1.1 eV (close to that of c-Si). To increase the efficiency beyond the Shockley-Queisser limit, two general approaches exist: adapt the solar cell or the solar spectrum. Successful (but costly) demonstration of the first approach is the tandem solar cell, where efficiencies up to 40% can be achieved by combining multiple semiconductor materials.[4,6] Other options may be efficient multiple-exciton generation (MEG), which was recently reported for various semiconductor nanocrystals (e.g., CdSe, PbSe, and PbS),[7] recently reported for silicon nanocrystals. Y_2O_3 is a promising host matrix for UC and quantum cutting because of its good chemical durability, thermal stability, and low phonon energy 400 cm^{-1}. Ho^{3+} has been investigated as one of the best UC luminescence activators for its high UC efficiency. Yb^{3+} ions is an ideal sensitizer for the Ho^{3+} ions, because they have a large absorption cross section around 980 nm and can efficiently transfer the excitation energy to Ho^{3+} ions[8].

Upconversion processes are only possible in trivalent lanthanide ions with metastable and long-lived intermediate levels acting as storage reservoirs for the pump energy.[9] In this sense, Er^{3+}, Tm^{3+}, and Ho^{3+} ions, featuring ladder-like energy levels for facilitating photon absorption and subsequent ET steps, were generally chosen as activators to give rise to efficient visible emissions under low pump power densities[10]. In order to enhance upconversion luminescence efficiency, the Yb^{3+} ion is usually co-doped as an excellent upconversion sensitizer due to its large absorption cross-section in the 900–1100 nm NIR region, corresponding to the $^2F_{5/2}$ - $^2F_{7/2}$ (Yb^{3+}) transition. The Ho^{3+} ion has a relatively wide absorption band in the 1150–1225 nm spectral range due to $^5I_8$-$^5I_6$ transition. The irradiation power density of sunlight in this spectral range is about 40 W $m^{-}2$, which is approximately twice more intense than that in the 1480–1580 nm range. Lahoz[11] in 2008 reported the use of Ho^{3+} singly-doped oxyfluoride glass ceramics as promising upconverters for efficiency enhancement in c-Si solar cells. In a following paper, Lahoz *et al.*[12] co-doped Ho^{3+} with Yb^{3+} and found enhanced emission intensity of NIR-to-NIR upconversion as a result of ET from Ho^{3+} to Yb^{3+} ions. On the other hand Ho^{3+}, Yb^{3+} codoped phosphor give the also quantum cutting phenomenon. The $^5F_3$ - $^5I_8$ transition of Ho^{3+} is approximately twice the energy required for the $^2F_{5/2}$ - $^2F_{7/2}$ transition of Yb^{3+}. However, the second-order cooperative quantum cutting process of [Ho^{3+} ($^5F_3$ - $^5I_8$); $2Yb^{3+}$ ($^2F_{7/2}$ - $^2F_{5/2}$)] is unlikely because the $^5F_3$ (Ho^{3+}) excited state can decay rapidly to the next $^5S_2$, $^5F_4$ states[14]. Lin and co-workers[13] first reported the first-order quantum-cutting luminescence for the Ho^{3+}–Yb^{3+} couple in glass ceramics with internal quantum efficiency of 159%. Under 488 nm blue-light excitation, Ho^{3+} could be excited to the $^5F_3$ state followed by nonradiative relaxation to $^5S_2$, $^5F_4$ states, from which the resonant cross-relaxation ET of [Ho^{3+} ($^5S_2$, $^5F_4$-$^5I_6$); Yb^{3+} ($^2F_{7/2}$ - $^2F_{5/2}$)] occurs. This leads to NIR quantum-cutting involving the emission of one 1180 nm photon ($^5I_6$ - $^5I_8$ transition of Ho^{3+}) and one 980 nm photon ($^2F_{5/2}$-$^2F_{7/2}$ transition of Yb^{3+}). In addition, some of the electrons in $^5S_2$,$^5F_4$ states of Ho^{3+} could further relax nonradiatively to the lower $^5F_5$ level, which induces another resonant cross-relaxation process of [Ho^{3+}($^5F_5$-$^5I_7$); Yb^{3+} ($^2F_{7/2}$-$^2F_{5/2}$)], and results in the intensity enhancement of Yb^{3+} emission[15]. The first-order NIR quantum-cutting for the Ho^{3+}–Yb^{3+} couple was later confirmed by Yu and co-workers in NaYF4 phosphors[16]. However, Deng *et al.*[17] proposed a different ET mechanism in these phosphors under ultraviolet (359 nm) excitation. They argued that the NIR quantum-cutting occurs at the 5G4 level, which involves two-step sequential cross relaxation: [Ho^{3+} ($^5G_4$-$^5F_5$); Yb^{3+} ($^2F_{7/2}$-$^2F_{5/2}$)] followed by [Ho^{3+} ($^5F_5$-$^5I_7$); Yb^{3+} ($^2F_{7/2}$ - $^2F_{5/2}$)]. Thus, one ultraviolet photon absorbed by Ho^{3+} gave rise to two NIR photons of Yb^{3+}, with a maximum quantum efficiency of 155.2%[18]. In this paper, we have synthesized Y_2O_3 doped Ho^{3+}, Yb^{3+} phosphor by solution method. The investigate the Ho^{3+},Yb^{3+} energy transfer processes at various Yb^{3+} concentrations (0 to 50 at%) and in Ho^{3+}(1 mol%) doped Y_2O_3. We investigate the X-ray diffraction, Scanning electron microscope (SEM), luminescence properties have been evaluated.

MATERIAL AND METHODS

The phosphor samples have been prepared by "complex based precursor solution method". For the preparation of samples, first of all, required amount of Yttrium Nitrate [$Y(NO_3)_3$], Holmium Nitrate [$Ho(NO_3)_3$] and Ytterbium Nitrate [$Yb(NO_3)_3$] were dissolved in double distilled water to prepare the stock solution of the metal nitrates respectively. In the next step, Y $(NO_3)_3$ and Ho/Yb $(NO_3)_3$ were taken in stoichiometric ratio in a beaker. This precipitate was in dissolved and a clear solution was obtained by adding a certain amount of concentrated nitric acid (HNO_3), maintaining the pH at 3–4. The clear solution of metal nitrate was then evaporated on a hot plate at 180^{o}C–200^{o}C with constant stirring. Continuous heating of the solution led to foaming and puffing powder is obtained. The precursor mass was then annealed at 1200^{o}C for 2 h to get the required samples.

RESULTS AND DISCUSSION

Structural characterizations: Initially, the phosphor sample was examined through XRD for structure and particle size. The XRD pattern of the phosphor shows the presence of crystalline cubic phase (JCPDS no.:25-1200) of Y_2O_3, which further do not show any change with a variation in Yb^{3+} concentration even up to 50 mol%, see Fig.1 (a). The material crystallises into cubic phase (a = b = c = 10.60 °A) with *Ia3* (206) space group. Yttrium (Y) ions are surrounded by six coordination to oxygen ions generating an assembly of two types of distorted YO_6 octahedra display in Fig.2 This confirms for an effective doping of Ho^{3+} and Yb^{3+} ions on Y^{3+} cite. On the other hand, transmission electron microscopy (TEM) image shows that the morphology of Y_2O_3 doped Ho^{3+}, Yb^{3+} is predominantly random in Fig.1 (b) which shows the presence of nanoparticles of average edge length 35 nm.

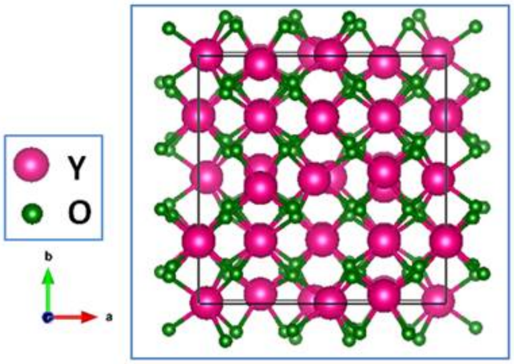

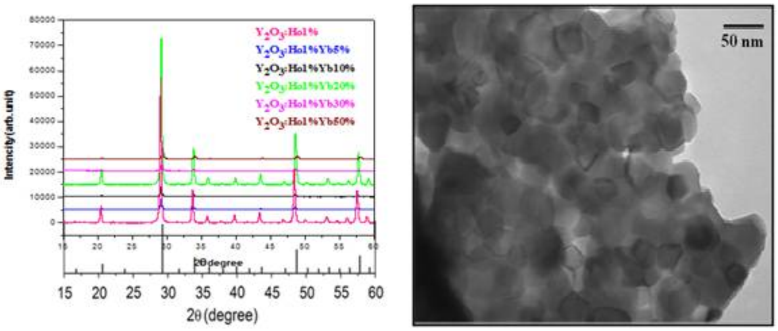

Figure 1: (a) XRD of Y2O3: Ho3+, Yb3+ phosphors and (b) TEM image of Y2O3:Ho3+, Yb3+ phosphor.
Figure 3: Crystal Structure of cubic Y2O3.

The emission spectra of the samples with λ_{exc} = 365 nm shown in Fig.4, respectively. PL spectrum also consists of several lines peaking at 536 nm, 549 nm, 656 nm, and 756 nm, corresponding to $^5F_{4/5} \rightarrow I_8$, $^5S_{2/5} \rightarrow I_8$, $^5F_{5/5} \rightarrow I_8$, and $^5S_{2/5} \rightarrow I_7$ transitions of the Ho^{3+} ion, respectively. The most intense peak is observed in green region at 549 nm. The Optimum concentration of Yb^{3+} is 5% then emission also decreases with increasing concentration of Yb^{3+}. Since, Yb^{3+} is known to have only one excited state ($^2F_{5/2}$) at around 10000 cm^{-1}, so, in principle there is no direct role of Yb^{3+} under UV excitations (362 nm and 449 nm). It is expected that this decrease in emission intensity, with an increase in Yb^{3+} concentration, could be due to an energy transfer from Ho^{3+} ions to Yb^{3+} ion.

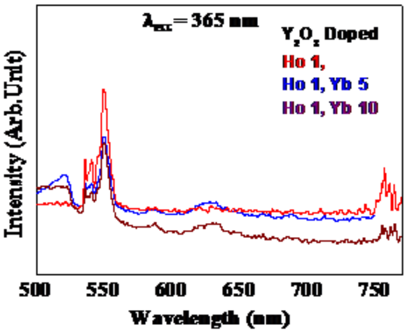

Figure 4: PL Emission spectra at λex = 365 nm, of Y2O3 doped with 1% Ho3+ x% Yb3+ (x= 0, 5, 10) phosphors.

To understand the DC mechanism in Ho^{3+} and Yb^{3+} codoped system in depth, the possible ET routes are presented in Fig.5 Excited by 365 nm wavelength, Ho^{3+} ion in the ground state $^5I_8$ is excited to $^5G_6/^5F_1$ state. Subsequently, $^5F_3$ level, $^5F_4/^5S_2$ level, and $^5F_5$ level can be populated by nonradiative relaxation processes from the corresponding upper state. Then, the Ho^{3+} in $^5F_{4/5}$-S^2 or $^5F_5$ state can transfer its energy to one nearby Yb^{3+} through cross-relaxation processes CR1 and CR2, respectively. Specially, the Ho^{3+}: $^5I_8 \rightarrow ^5F_3$ transition is located at approximately twice the energy of the Yb^{3+}: $^2F_{5/2} \rightarrow ^2F_{7/2}$ transition and the position of $^5I_5$ state of Ho^{3+} is a little higher than that of $^2F_{5/2}$ state of Yb^{3+}. In addition, Yb^{3+} has no other levels up to the UV region. Therefore, the ET from Ho^{3+} in $^5F_3$ level to Yb^{3+} has two possible routes: (a) two-step ET, as shown in Fig 5: the first ET step is that the Ho^{3+} ion in 5F3 level transfers its energy to one Yb^{3+} ion through CR3 [5F3 (Ho^{3+}) + $^2F_{7/2}$ (Yb^{3+})$\rightarrow$$^5I_5$ (Ho^{3+}) + $^2F_{5/2}$ (Yb^{3+})]; next, the second ET step is that the Ho^{3+} ion in $^5I_5$ level is de-excited to the ground state and then transfers its energy to another Yb^{3+} ion [$^5I_5$ (Ho^{3+}) + $^2F_{7/2}$ (Yb^{3+}) $\rightarrow$$^5I_8$ (Ho^{3+}) + $^2F_{5/2}$ (Yb^{3+})]. (b) Cooperative ET (CET), as shown in Fig 5: two Yb^{3+} ions in the ground state are simultaneously excited to $^2F_{5/2}$ state by receiving energy from the same Ho^{3+} ion in $^5F_3$ level.

CONCLUSION

Ho^{3+}/Yb^{3+} co-doped yttrium oxide phosphors have been synthesized, the phase analysis by powder XRD, measurement of SEM images, Steady State and Time Resolved Photoluminescence Study has been investigated in detail. An cubic of Y_2O_3:Ho^{3+},Yb^{3+} phosphor show a pure phase by X-Ray diffraction and Photoluminescence emission (PL) spectra, reveals the efficient emission in the green region which corresponds to $^5S_2$–$^5I_8$ transition of Ho^{3+}.The energy transfer from Ho^{3+} to Yb^{3+} has been calculated, whose efficiency is around 72.91%, and so, the corresponding QC efficiency is 172.91%.

REFERENCES

1. O. Morton, Nature (2003), 443, 19.
2. B. van der Zwaan, A. Rabl, Sol. Energy (2003), 74, 19.

3. B. S. Richards, Sol. Energy Mater. Sol. Cells (2006), 90, 2329.
4. M. A. Green, Physica E (2002), 14, 11.
5. W. Shockley, H. J. Queisser, J. Appl. Phys. (1961), 32, 510.
6. S. Kurtz, D. Friedman, J. Geisz, W. McMahon, J. Cryst. Growth (2007), 298,748.
7. R. D. Schaller, V. M. Agranovich, V. I. Klimov, Nat. Phys. (2005), 1, 189.
8. WEI Xiantao, LI Yong, CHENG Xuerui, CHEN Yonghu, YIN Min, JOURNAL OF RARE EARTHS, Vol. 29, 536, (2011).
9. F. Wang and X. G. Liu, Chem. Soc. Rev., 38, 976–989,(2009).
10. F. Auzel, Chem. Rev., 104, 139–173 (2004).
11. F. Lahoz, Opt. Lett.33, 2982–2984, (2008).
12. F. Lahoz, C. Perez-Rodriguez, S. E. Hernandez, I. R. Martin, V. Lavin and U. R. Rodriguez-Mendoza, Sol. Energy Mater. Sol. Cells, 95, 1671–1677, (2011).
13. X. P. Chen, W. J. Zhang and Q. Y. Zhang, Physica B (Amsterdam), 406, 1248–1252 (2011).
14. H. Lin, D. Chen, Y. Yu, A. Yang and Y. Wang, Opt. Lett. 36, 876–878 (2011).
15. D. C. Yu, X. Y. Huang, S. Ye and Q. Y. Zhang, J. Alloys Compd. 509, 9919–9923(2011).
16. K. Deng, T. Gong, L. Hu, X. Wei, Y. Chen and M. Yin, Opt. Express, 19, 1749–1754 (2011).
17. R. V. Yadav, S. K. Singh and S. B. Rai RSC Adv., 5, 26321 (2015).
18. A. Pandey and V. K. Rai, Dalton Trans. 42, 11005–11011 (2013).
19. X. Huang, S. Han, W. Huang and X. Liu, Chem. Soc. Rev., 42, 173–201 (2013).

Source of Support: None Declared
Conflict of Interest: None Declared